

Physical Chemistry of the Reduction of Calcium Oxide with Aluminum in Vacuum

K.T. Jacob and S. Srikanth

*Department of Metallurgy, Indian Institute of Science
Bangalore 560 012, India*

CONTENTS

ABSTRACT

	Page
ABSTRACT	77
1. INTRODUCTION	78
2. THERMODYNAMIC BASIS OF "ALUMINOTHERMIC" REDUCTION OF CALCIUM OXIDE IN VACUUM	78
3. PHYSICAL CHEMISTRY OF "ALUMINOTHERMIC" REDUCTION	79
3.1. Thermodynamic Data on Liquid Al-Ca Alloys	79
3.2. Gibbs Energy of Formation of Calcium Aluminates	80
3.3. Stages in the Reduction of CaO with Al	82
3.4. Equilibrium Alloy Compositions and Oxygen Potentials	83
3.5. Vapor Pressure Measurement and Calculation	84
4. CHARGE AND ENTHALPY CALCULATIONS	87
5. PURITY OF CALCIUM	88
6. PROCESS CONTROL	88
6.1. Kinetics of the Process	90
6.2. Plant Practice	90
7. DISCUSSION AND CONCLUSIONS	91
8. REFERENCES	92

The physical chemistry of "aluminothermic" reduction of calcium oxide in vacuum is analyzed. Basic thermodynamic data required for the analysis have been generated by a variety of experiments. These include activity measurements in liquid Al-Ca alloys and determination of the Gibbs energies of formation of calcium aluminates. These data have been correlated with phase relations in the Ca-Al-O system at 1373 K. The various stages of reduction, the end products and the corresponding equilibrium partial pressures of calcium have been established from thermodynamic considerations. In principle, the recovery of calcium can be improved by reducing the pressure in the reactor. However,, the cost of a high vacuum system and the enhanced time for reduction needed to achieve higher yields makes such a practice uneconomic. Aluminum contamination of calcium also increases at low pressures. The best compromise is to carry the reduction up to the stage where $3\text{CaO}\cdot\text{Al}_2\text{O}_3$ is formed as the product. This corresponds to an equilibrium calcium partial pressure of 31.3 Pa at 1373 K and 91.6 Pa at 1460 K. Calcium can be extracted at this pressure using mechanical pumps in approximately 8 to 15 hr, depending on the size and the fill ratio of the retort and porosity of the charge briquettes.

1. INTRODUCTION

Calcium and its alloys are important for nuclear technology, defense applications, ferrous and nonferrous metallurgy. Calcium is widely used for the extraction of nuclear materials such as uranium and thorium by calciothermic reduction of their halides. The hydride of calcium is a strategic defense material used for hydrogen generation. In ferrous and nonferrous metallurgy, calcium is used as a powerful deoxidizer, as an alloying element to improve the quality of ferrous castings and hot workability of Al-Cu-Mg alloys. Calcium is used for diffusion barrier coatings on stainless steels and clad steels to improve their wear resistance. Calcium spun wires are used in specialized electrical instruments requiring high electrical conductivity characteristics.

The common routes for the production of metallic calcium are the electrolysis of fused calcium chloride and "aluminothermic" reduction of calcia in vacuum. Prior to the Second World War, production of calcium was mainly by the electrolytic route, but presently it is almost entirely by the reduction of calcium oxide with aluminum. Among the disadvantages of the electrolytic process are the difficulty in production of pure anhydrous calcium chloride, solubility of lime and calcium in calcium chloride, low yield of calcium and susceptibility of calcium to oxidation. The "aluminothermic" reduction of lime in vacuum has been found to be the most economically viable route, especially when volume of production is low. Calcium production by the two commercial producers in North America is estimated to be in excess of 450 tons per year /1/. The process is similar to the Pidgeon process for the production of magnesium. However, the reduction of calcia by aluminum is endothermic and, strictly speaking, it is not an aluminothermic reduction. In this process, high-grade limestone is first crushed, pulverized and calcined. The calcined powders are briquetted with aluminum powder and the briquettes are then thermally processed under vacuum in horizontal retort furnaces at temperatures in the range of 1373-1460 K. The calcium vapors produced by the reduction of CaO are condensed on special alloy steel condensers. The reaction is highly endothermic and a large amount of heat has to be supplied. Crude calcium so produced is stripped from the condenser and stored in an argon atmosphere. Finally, the normal 99% pure product is redistilled to enhance purity.

During the "aluminothermic" reduction process, a Ca-Al alloy is formed which decreases the efficiency of utilization of aluminum and recovery of calcium. The major drawbacks of the "aluminothermic" reduction of calcia are the high energy consumption, the low recovery of calcium and some loss of the expensive reductant, Al. A thermodynamic analysis of the process is useful for process optimization. In this paper, recent thermodynamic data on systems of interest to "aluminothermic" reduction are reviewed, and the sequence of reaction and the vapor pressure of calcium corresponding to each step of the reduction process are presented. Charge and enthalpy balance for the process are outlined. Finally, economically optimum conditions for commercial operation are suggested.

2. THERMODYNAMIC BASIS OF "ALUMINOTHERMIC" REDUCTION OF CALCIUM OXIDE IN VACUUM

Special methods are necessary to reduce very stable oxides such as CaO since no simple reduction reaction is apparent from the Ellingham diagram for oxides. The oxygen potentials corresponding to the coexistence of Ca, Al and C with their oxides are plotted in Fig. 1. Thermodynamic data for the free energies of formation of CaO, Al₂O₃ and CO and auxiliary data for the enthalpy and entropy of fusion of pure calcium and aluminum were taken from JANAF thermochemical tables /2,3/. Vapor pressure of pure calcium was based on the studies of Jacob *et al.* /4/. The thermal dissociation of calcium oxide can be accomplished only at temperatures above 4000 K. Since suitable container materials are not available at such high temperatures, this process is clearly not practical. From the Ellingham diagram it is seen that calcia can be directly reduced by carbon above 2400 K at a total pressure of 1 atm (10⁵ Pa). The temperature for reduction can be lowered by operating under reduced pressure. However, the formation of calcium carbide makes this process unattractive and, in addition, the process is associated with large energy consumption and high refractory losses. An alternate procedure for the reduction of calcia is to employ metallic reducing agents. The only common metal which can be used as a reductant for calcium oxide is aluminum because the oxides of other common metals are much less

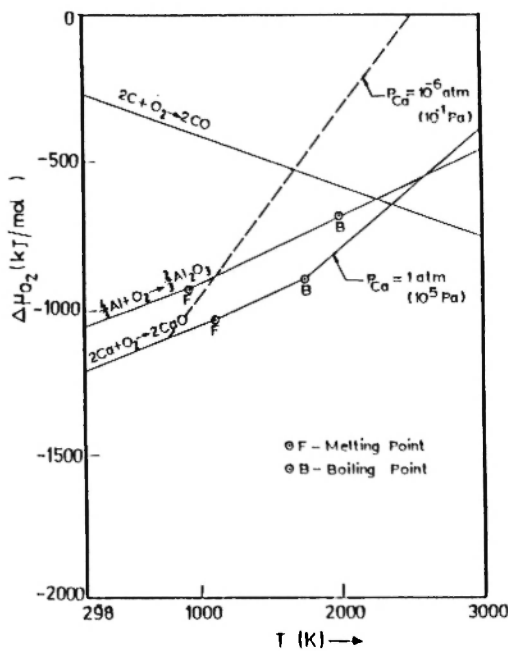
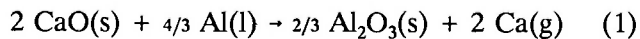


Fig. 1: Ellingham diagram for oxides of Ca, Al and C.

stable than calcia at all temperatures. "Aluminothermic" reduction of calcia can be represented by the reaction:



From Fig. 1 it is seen that this hypothetical reaction becomes feasible at ~2600 K at 1 atm (10^5 Pa) pressure. However, if the pressure in the reactor is reduced to 10^{-6} atm (10^{-1} Pa), the free energy change for the reduction is lowered by an amount equal to $2.3(12RT)$. Thus, the equilibrium temperature for "aluminothermic" reduction of calcium oxide drastically reduces to ~1140 K if a vacuum of the order of 10^{-6} atm (10^{-1} Pa) is employed.

3. PHYSICAL CHEMISTRY OF "ALUMINOTHERMIC" REDUCTION

The products of "aluminothermic" reduction are not pure calcium and aluminum oxide as depicted in Eq. 1, since liquid aluminum absorbs calcium to form an Al-Ca alloy. The CaO-Al₂O₃ pseudo-binary system contains five compounds [5]. Pure Al₂O₃ cannot coexist in stable equilibrium with CaO. A knowledge of activities in liquid Al-Ca alloys, data on the free

energy and enthalpy of formation of calcium aluminates, as well as vapor pressure of calcium and the alloy compositions corresponding to different possible reduction equilibria, are of interest to the physical chemistry of "aluminothermic" reduction of calcium oxide in vacuum.

3.1. Thermodynamic Data on Liquid Al-Ca Alloys

Enthalpies of mixing in liquid Al-Ca alloys have been measured by Sommer *et al.* [6] by calorimetry in the temperature range 980-1190 K. The enthalpies are negative and independent of temperature over the entire concentration range (Fig. 2). Activities in liquid Al-Ca alloys have been measured by Jacob *et al.* [4] utilizing the Knudsen effusion technique and distribution measurements at 1373 K. Activities in liquid alloys have also been measured by Schurmann *et al.* [7] using a boiling point method at 1623 K. The activity-composition curves depicting the results of Jacob *et al.* and Schurmann *et al.* are compared in Fig. 3. Although these results are in qualitative agreement, indicating approach to ideality with increasing temperature, the temperature dependence of activity is not fully consistent with the enthalpies

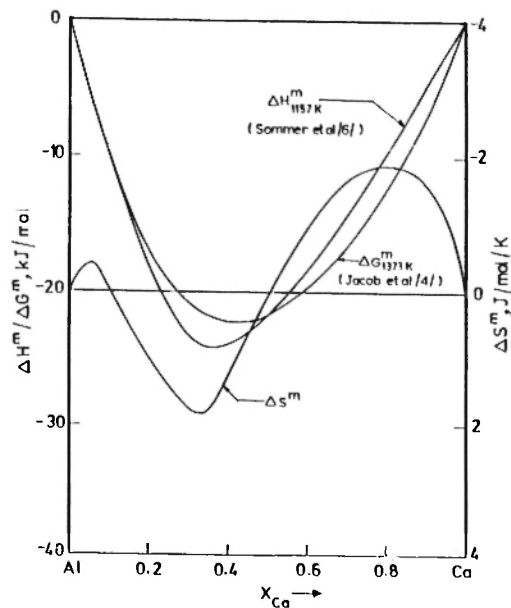


Fig. 2: Free energy (1373 K), enthalpy and entropy of mixing for liquid Al-Ca alloys.

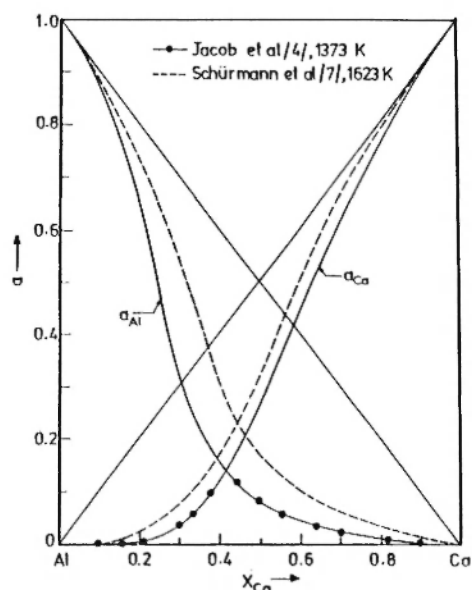


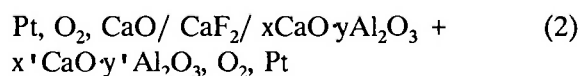
Fig. 3: Composition dependence of activities in liquid Al-Ca alloys.

of mixing reported by Sommer *et al.* /6/. Since "aluminothermic" reduction of calcia is carried out at about 1400 K, the activity data of Jacob *et al.* /4/ at 1373 K are more relevant for process analysis. Entropy of mixing obtained by combining the results of Jacob *et al.* /4/ with the calorimetric measurements of Sommer *et al.* /6/ are also shown in Fig. 2.

3.2. Gibbs Energy of Formation of Calcium Aluminates

Early literature on the thermodynamics of the system CaO-Al₂O₃ are summarized in reviews by Chipman /8/ and Rein and Chipman /9/. These reviews identify two important sets of thermodynamic data: the heat capacity and heat of formation of CaO·2Al₂O₃, CaO·Al₂O₃, 12CaO·7Al₂O₃ and 3CaO·Al₂O₃ reported by Koehler *et al.* /10/; and activity measurements of Sharma and Richardson /11/ in the liquid state, later confirmed and extended by Kor and Richardson /12/. These two sets of data are not compatible for the composition corresponding to CaO·2Al₂O₃ and CaO·Al₂O₃. Activities derived by Carter and Macfarlane /13/ are based on an incorrect assumption regarding the constancy of the activity coefficient of CaS in the melts. Measurements by Cameron *et al.* /14/ on

sulfide solubilities are incompatible with those of Kor and Richardson /12/ and with thermochemical data /10/ on 12CaO·7Al₂O₃ and 3CaO·Al₂O₃. Thermochemical information on the compound CaO·6Al₂O₃ was not available from the early studies. More recent measurements on the system CaO-Al₂O₃ are due to Allibert *et al.* /15/ and Kumar and Kay /16/. Allibert *et al.* attempted to measure the standard free energies of formation of solid calcium aluminates from their component oxides in the temperature range 923-1123 K using a solid state cell incorporating single crystal CaF₂ as the solid electrolyte. Their cell can be schematically represented as



The right-hand electrode contains two adjoining oxide phases in the pseudobinary system CaO-Al₂O₃. The emfs can be related unambiguously to thermodynamic data for the compounds CaO·6Al₂O₃, CaO·2Al₂O₃ and, perhaps, CaO·Al₂O₃. Due to the probable formation of a solid solution between 12CaO·7Al₂O₃ and 11CaO·7Al₂O₃·CaF₂ at the electrode/electrolyte interface, emf studies cannot be relied on for obtaining data for the compounds 12CaO·7Al₂O₃ and 3Ca·Al₂O₃. Phase relations in the Al₂O₃-CaO-CaF₂ system at 1373 K /17/ are illustrated in Fig. 4A. Allibert *et al.* /15/ have also measured activities in CaO-Al₂O₃ melts at 2060 K using Knudsen effusion mass spectrometry. The data recommended by Allibert *et al.* for the Gibbs energy of formation of 12CaO·7Al₂O₃ and 3CaO·Al₂O₃ were based on thermal data /10/ as well as activities in CaO-Al₂O₃ melts /11,15/, taken in conjunction with the phase diagram. The temperature dependence of activities in the CaO-Al₂O₃ melts were calculated by Allibert *et al.* /15/ by combining the results of their mass spectrometric study at 2060 K with those of Sharma and Richardson /11/ at 1773 K. Values recommended for the free energies of formation of the interoxide compounds CaO·6Al₂O₃, CaO·2Al₂O₃ and CaO·Al₂O₃ from component oxides were based on a critical evaluation of their own measurements and those reported earlier in the literature /8-10,12/. Activities in liquid phase were correlated with the Gibbs energy of formation of solid compounds and the phase diagram. The recommended values for the free energies of formation of the various aluminates in the system

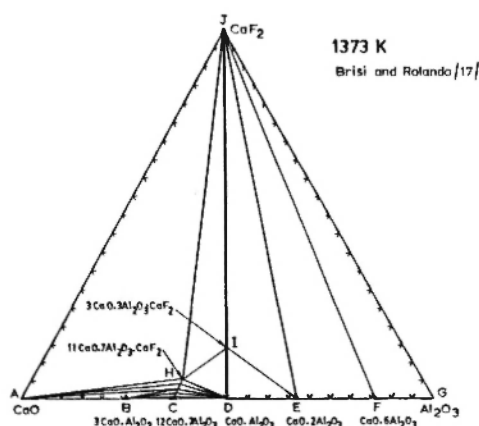


Fig. 4A: Phase diagram of the system $\text{CaO}-\text{Al}_2\text{O}_3-\text{CaF}_2$ at 1373 K.

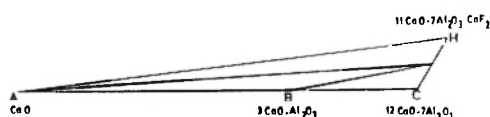


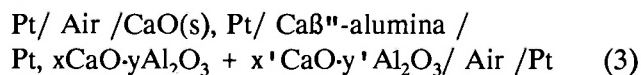
Fig. 4B: Expanded picture of the three-phase region $\text{CaO} + 3\text{CaO}\cdot\text{Al}_2\text{O}_3 + (11+x)\text{CaO}\cdot(1-x)\text{CaF}_2\cdot 7\text{Al}_2\text{O}_3$ (section ACH in Fig. 4A).

$\text{CaO}-\text{Al}_2\text{O}_3$ from component oxides are given in Table 1 as a function of temperature.

TABLE 1
Free Energies of Formation of the Inter-oxide Compounds in the System $\text{Al}-\text{Ca}-\text{O}$
(Based on the Data of Allibert *et al.* /15/)

Compound	ΔG° , kJ/mol	
	(from component oxides)	ΔG° 1373, kJ/mol (from elements)
CaO(s)	--	-486.884
$\text{Al}_2\text{O}_3(\text{s})$	--	-1238.075
$\text{CaO}\cdot 6\text{Al}_2\text{O}_3(\text{s})$	$-17.43 - 0.0372 T$	-7983.840
$\text{CaO}\cdot 2\text{Al}_2\text{O}_3(\text{s})$	$-16.40 - 0.0268 T$	-3016.230
$\text{CaO}\cdot \text{Al}_2\text{O}_3(\text{s})$	$-18.12 - 0.0186 T$	-1768.644
$12/7 \text{ CaO}\cdot \text{Al}_2\text{O}_3$	$-12.30 - 0.0293 T$	-2125.262
$3\text{CaO} \cdot \text{Al}_2\text{O}_3$	$-17.00 - 0.0320 T$	-2759.663

Kumar and Kay /16/ employed a solid-state electrochemical technique with CaB'' -alumina as the electrolyte for the determination of the free energies of formation of the aluminate phases, $\text{CaO}\cdot 6\text{Al}_2\text{O}_3$, $\text{CaO}\cdot 2\text{Al}_2\text{O}_3$, $\text{CaO}\cdot \text{Al}_2\text{O}_3$ and $3\text{CaO}\cdot \text{Al}_2\text{O}_3$, from component oxides in the temperature range 1050-1500 K. Their emf cells can be schematically represented as



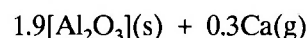
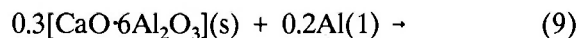
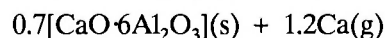
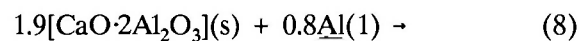
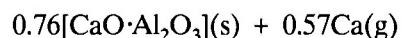
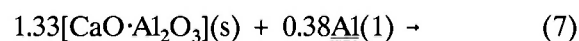
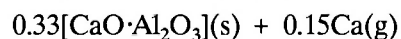
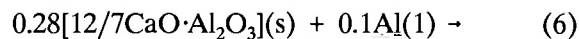
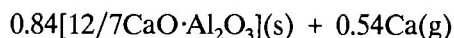
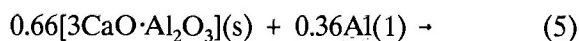
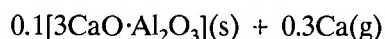
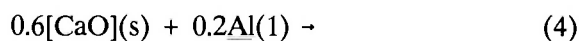
where the right-hand electrode contains a mixture of adjoining phases in the $\text{CaO}-\text{Al}_2\text{O}_3$ system. Their results suggest lower stabilities for the compounds $\text{CaO}\cdot 2\text{Al}_2\text{O}_3$, $\text{CaO}\cdot \text{Al}_2\text{O}_3$ and $3\text{CaO}\cdot \text{Al}_2\text{O}_3$ compared to the values recommended by Allibert *et al.* /15/, whereas for the compound $\text{CaO}\cdot 6\text{Al}_2\text{O}_3$, Kumar and Kay /16/ suggest lower values for the free energy of formation. Kumar and Kay employed a CaO reference electrode in contact with CaB'' -alumina electrolyte. The phase diagram clearly indicates that the alumina-rich CaB'' -alumina cannot coexist with CaO . Their electrolyte/reference electrode interface is therefore thermodynamically unstable, raising doubts on the validity of their data. They also ignore the existence of the compound $12\text{CaO}\cdot 7\text{Al}_2\text{O}_3$ and attribute traces of this phase in their samples to the presence of moisture. The phase diagram of the system $\text{CaO}-\text{Al}_2\text{O}_3$ by Levin *et al.* /5/ shows five interoxide compounds including $12\text{CaO}\cdot 7\text{Al}_2\text{O}_3$. The more recent phase diagram by Nurse *et al.* /18/, however, shows that $12\text{CaO}\cdot 7\text{Al}_2\text{O}_3$ is not stable in the pseudobinary system $\text{CaO}-\text{Al}_2\text{O}_3$. Nurse *et al.* /18/ suggest that this phase is stabilized by moisture or halogens. However, Cockayne and Lent /19/ have grown single crystals of $12\text{CaO}\cdot 7\text{Al}_2\text{O}_3$ several centimeters long from melts. An infrared adsorption band at $2.8 \mu\text{m}$ due to hydroxyl ions was observed in their sample, but since the adsorption was unaffected by prolonged vacuum treatment of the melt, it is likely that the OH^- ions are present as an impurity rather than as a constituent. Srikanth *et al.* /20/ have also found $12\text{CaO}\cdot 7\text{Al}_2\text{O}_3$ to coexist with $\text{Al}-\text{Ca}$ alloys. Since H_2O would be unstable in the presence of these alloys, this finding suggests that the compound is stable even in the absence of moisture.

Values for the free energies of formation of the interoxide compounds in the pseudobinary system $\text{CaO}-\text{Al}_2\text{O}_3$ selected for the present analysis are those

of Allibert *et al.* /15/. Free energies of formation of calcia and alumina are listed in JANAF thermochemical tables /2,3/. However, Srikanth and coworkers /20/ suggest that the free energy of formation of CaO may be slightly more positive than the value reported in JANAF /3/. In their alloy-oxide equilibration studies in the system Al-Ca-O, they obtain a better agreement between the computed and experimental alloy compositions if the standard Gibbs energy of formation of CaO is taken to be -487.0 kJ/mol compared to the value of -491.2 kJ/mol suggested in JANAF /3/ at 1373 K. Hence, in the present analysis, the free energy of formation of Al_2O_3 was taken from JANAF /2/ and the Gibbs energy of formation of CaO was taken as 4.2 kJ/mol, more positive than the values given by JANAF /3/. The computed free energies of formation of the aluminate phases from elements are listed in Table 1.

3.3. Stages in the Reduction of CaO with Al

The probable reactions in the "aluminothermic" reduction of calcia are



The reductant Al is generally not present at unit activity; it absorbs calcium to form an Al-Ca alloy. The phase rule indicates that each of the above reactions involving three condensed phases and a gas phase is associated with one degree of freedom—either the temperature or pressure can be varied to control the reaction. The reactant and product oxides can be in stable equilibrium only if they are the adjacent phases in the system CaO- Al_2O_3 . Since seven stable oxides exist in the system CaO- Al_2O_3 including the end members and only two adjacent oxides can be in stable equilibrium, six different stages are possible in the reduction of calcia. The free energy change at 1373 K for each equilibrium is contained in Table 2 along with the equilibrium constant or activity ratio characterizing each reaction.

TABLE 2
Standard Free Energy Changes and Equilibrium Constant Characterizing the Reduction Stages in the "Aluminothermic" Reduction of Calcia at 1373 K

Equilibrium	ΔG_{1373}° (kJ)	$K = \frac{p_{\text{Ca}}^x}{a_{\text{Al}}^y}$
$0.6[\text{CaO}](s) + 0.2\text{Al}(1) \rightarrow 0.1[3\text{CaO} \cdot \text{Al}_2\text{O}_3](s) + 0.3\text{Ca}(g)$	26.65	0.0968
$0.66[3\text{CaO} \cdot \text{Al}_2\text{O}_3](s) + 0.36\text{Al}(1) \rightarrow 0.84[12/7\text{CaO} \cdot \text{Al}_2\text{O}_3](s) + 0.54\text{Ca}(g)$	55.04	0.0081
$0.28[12/7\text{CaO} \cdot \text{Al}_2\text{O}_3](s) + 0.1\text{Al}(1) \rightarrow 0.33[\text{CaO} \cdot \text{Al}_2\text{O}_3](s) + 0.15\text{Ca}(g)$	16.66	0.2323
$1.33[\text{CaO} \cdot \text{Al}_2\text{O}_3](s) + 0.38\text{Al}(1) \rightarrow 0.76[\text{CaO} \cdot 2\text{Al}_2\text{O}_3](s) + 0.57\text{Ca}(g)$	79.89	9.131×10^{-4}
$1.9[\text{CaO} \cdot 2\text{Al}_2\text{O}_3](s) + 0.8\text{Al}(1) \rightarrow 0.7[\text{CaO} \cdot 6\text{Al}_2\text{O}_3](s) + 1.2\text{Ca}(g)$	184.11	9.896×10^{-8}
$0.3[\text{CaO} \cdot 6\text{Al}_2\text{O}_3](s) + 0.2\text{Al}(1) \rightarrow 1.9[\text{Al}_2\text{O}_3](s) + 0.3\text{Ca}(g)$	53.30	0.0094

3.4. Equilibrium Alloy Compositions and Oxygen Potentials

In the "aluminothermic" reduction of calcia, aluminum dissolves calcium vapor to form a liquid Al-Ca alloy. For the analysis of the process, it is useful to know the equilibrium compositions of the alloy coexisting with different oxide phases at equilibrium. The equilibrium alloy compositions have been determined empirically and by thermodynamic computation.

Srikanth and coworkers /20/ have determined the equilibrium alloy compositions coexisting with the various oxide phases at 1373 K by equilibration in a closed cell. They have identified the equilibrium oxide phases by x-ray diffraction and determined the alloy compositions by chemical analysis. The primary oxide phases in contact with the alloy and the equilibrium compositions of the alloy obtained in their study at 1373 K are summarized in Table 3. The tie lines delineating equilibria between the different oxides and liquid Al-Ca alloys in the system Al-Ca-O at 1373 K are shown in Fig. 5.

The alloy composition corresponding to each equilibrium in the reduction process, determined by thermodynamic calculations using the free energies of formation of the various aluminates (Table 1) and activity data on liquid Al-Ca alloys /4/, are also listed in Table 3. A graphical procedure was adopted for determining the equilibrium alloy compositions

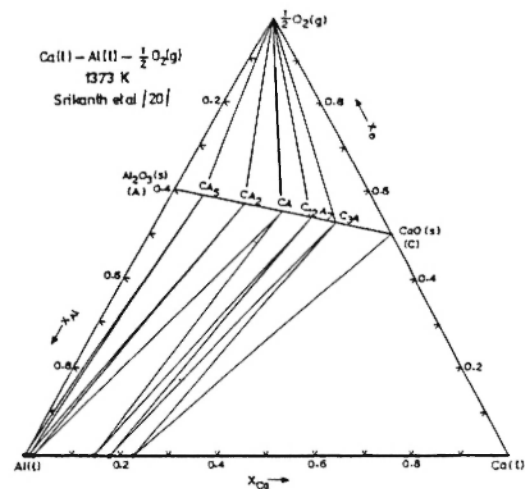


Fig. 5: Phase diagram of the Al-Ca-O system showing the tie lines between the alloy and oxide phases at 1373 K.

coexisting with the oxide phases. The computed alloy compositions are in very good agreement with the experimental results of Srikanth *et al.* /20/. Equilibrium alloy compositions coexisting with the oxide phases in the CaO-Al₂O₃ system determined using the data of Kumar and Kay /16/ for the aluminate phases and the alloy data of Jacob *et al.* /4/, compare less favorably with the experimental phase diagram /20/.

The oxygen partial pressures corresponding to the

TABLE 3
Equilibrium Alloy Compositions and Coexisting Oxide Phases in the Al-Ca-O System at 1373 K /20/

Coexisting Oxide Phases	Equilibrium Alloy Composition (X_{Ca})	
	Experimental	Thermodynamic Calculation
$Al_2O_3 + CaO \cdot 6Al_2O_3$	0.00096	0.00095
$CaO \cdot 6Al_2O_3 + CaO \cdot 2Al_2O_3$	0.0061	0.0057
$CaO \cdot 2Al_2O_3 + CaO \cdot Al_2O_3$	0.016	0.015
$CaO \cdot Al_2O_3 + 12/7 CaO \cdot Al_2O_3$	0.146	0.144
$12/7 CaO \cdot Al_2O_3 + 3CaO \cdot Al_2O_3$	0.173	0.176
$3CaO \cdot Al_2O_3 + CaO$	0.222	0.223

various three-phase and two-phase equilibria in the system Al-Ca-O can be computed from a knowledge of the equilibrium tie line compositions, free energies of formation of calcium aluminates and activities in liquid Al-Ca alloys. The computed oxygen potential diagram for the Al-Ca-O system at 1373 K depicting the variation of oxygen potential with molar ratio of metallic components ($n_{\text{Ca}}/n_{\text{Ca}} + n_{\text{Al}}$) is displayed in Fig. 6. The oxygen partial pressure regimes for the existence of different phases or phase mixtures can be readily read from the diagram. This diagram obeys the same topological construction rules as the conventional temperature-composition diagram. When three condensed phases coexist at a specified temperature, the system is invariant. The oxygen partial pressure is a function of composition in two-phase fields. The main disadvantage of the oxygen potential diagram is its inability to display the oxygen nonstoichiometry of the phases. However, since all the interoxide compounds in the system Al-Ca-O are nearly stoichiometric, it is not a serious limitation in the present case.

3.5. Vapor Pressure Measurement and Calculation

Vapor pressure of calcium over pure liquid calcium as a function of temperature (900-1400 K) and over Al-Ca alloys at 1373 K has been measured by Jacob

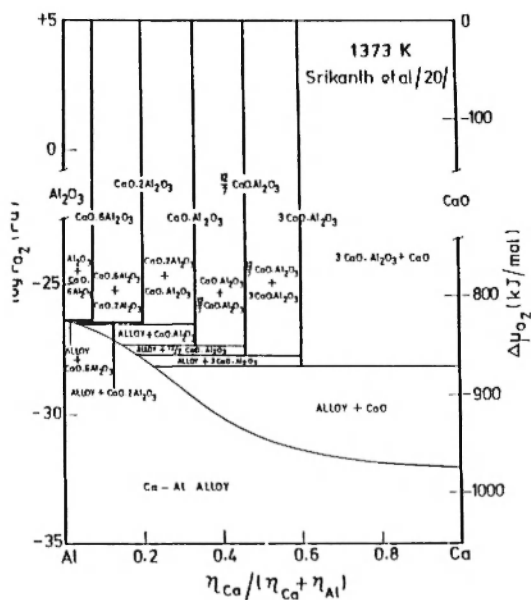
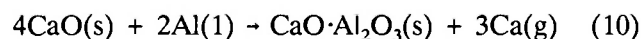


Fig. 6: Oxygen potential diagram for the Al-Ca-O system at 1373 K.

et al. /4/ using the Knudsen effusion technique. Vapor pressure of pure calcium as a function of reciprocal of absolute temperature is shown in Fig. 7 in comparison to the recommended values of Hultgren *et al.* /21/. Enthalpy and entropy of vaporization of liquid calcium derived from the vapor pressure studies of Jacob *et al.* /4/ are in good agreement with the recommended values /3,21/.

Atkinson and Pidgeon /22/ in their discussion of the thermodynamic aspects of aluminothermic reduction of calcium oxide suggest that the primary reaction in the process is



However, their designation of end product was not based on direct evidence. They used a modified form of the effusion method to measure vapor pressures of calcium corresponding to this equilibrium at various temperatures. They collected the vapor effusing from the orifice of the cell on a water cooled steel condenser and determined the rates of effusion from weight of the condensate. From the earlier discussion on phase stability, it is clear that the phase

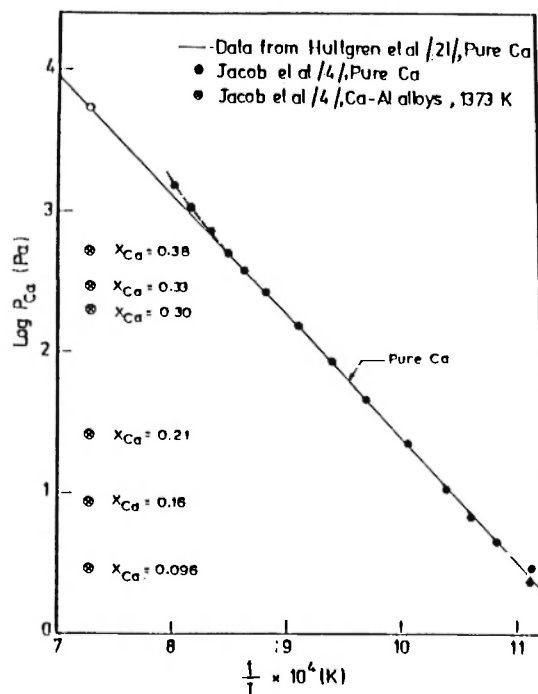
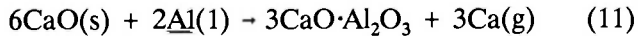
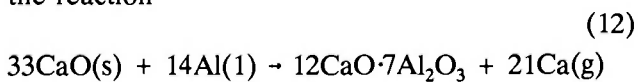


Fig. 7: Variation of the logarithm of the saturation vapor pressure of calcium over the pure metal with the reciprocal of absolute temperature. The partial pressure of calcium over Al-Ca alloys at 1373 K is also shown.

$\text{CaO} \cdot \text{Al}_2\text{O}_3$ cannot be in equilibrium with CaO . Only $3\text{CaO} \cdot \text{Al}_2\text{O}_3$ can coexist in equilibrium with CaO . In light of the present knowledge on phase relations in the $\text{Al}-\text{Ca}-\text{O}$ system, the partial pressures of calcium measured by Atkinson and Pidgeon /22/ probably correspond to the equilibrium

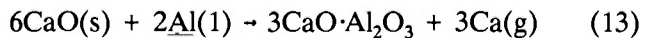


Their measured vapor pressures were used to derive an analytical expression for $\log p_{\text{Ca}}$ as a function of $1/T$ using the least-square regression analysis. The results are indicated in Table 4. Bauer /23/ claims to have determined the vapor pressure of calcium by Knudsen effusion as a function of temperature for the reaction



This equilibrium is again not in accord with the phase diagram. Bauer added small quantities of CaF_2 to CaO for catalyzing the "aluminothermic" reaction. The presence of CaF_2 leads to the stabilization of the phase $12\text{CaO} \cdot 7\text{Al}_2\text{O}_3$. Phase relations in the Al_2O_3 - $\text{CaO}-\text{CaF}_2$ system at 1373 K (Fig. 4A) indicate that the initial product of reduction of CaO with Al in the presence of a few percent of CaF_2 will lie in the three-phase field $[\text{CaO} + 3\text{CaO} \cdot \text{Al}_2\text{O}_3 + (11+x)\text{CaO} \cdot (1-x)\text{CaF}_2 \cdot 7\text{Al}_2\text{O}_3]$ close to the two-phase tie line between CaO and $(11+x)\text{CaO} \cdot$

$(1-x)\text{CaF}_2 \cdot 7\text{Al}_2\text{O}_3]$. The expanded picture of the three-phase region $[\text{CaO} + 3\text{CaO} \cdot \text{Al}_2\text{O}_3 + (11+x)\text{CaO} \cdot (1-x)\text{CaF}_2 \cdot 7\text{Al}_2\text{O}_3]$ is shown in Fig. 4B. The concentration of $3\text{CaO} \cdot \text{Al}_2\text{O}_3$ in the product will be small, perhaps below the detection limit by x-ray diffraction, during the early phase of the reaction. In the Knudsen cell reaction proceeds to only a limited extent during the time of measurement. If this reaction were allowed to proceed further, then the relative concentration of $3\text{CaO} \cdot \text{Al}_2\text{O}_3$ will increase in the product. The vapor pressure of Ca corresponding to reaction (12) obtained by Bauer /23/ is given in Table 4. In view of the uncertainty of the end products in the studies of Atkinson and Pidgeon /22/ and of Bauer /23/, new measurements were undertaken by Jacob and Srikanth /224/ to measure vapor pressure of calcium as a function of temperature corresponding to the equilibrium



Jacob and Srikanth /24/ used Knudsen effusion and weight loss analysis to measure vapor pressures of calcium in the temperature range 1190-1500 K. Their results are displayed in Table 4 and Fig. 8. The vapor pressure of calcium obtained by Jacob and Srikanth /24/ for reaction (13) is close to that of Bauer /23/ for reaction (12), when experimental uncertainties are taken into account. The associated enthalpy and

TABLE 4
Vapor Pressure Relations, Enthalpy and Entropy for the Different Reduction Mechanisms

Reaction	Vapor Pressure Relation (p_{Ca} in Pa and T in K)	ΔH kJ	ΔS J/K	Investigator
$4\text{CaO(s)} + 2\text{Al(1)} = \text{CaO} \cdot \text{Al}_2\text{O}_3 + 3\text{Ca(g)}$	$\log p_{\text{Ca}} = \frac{-5795}{T} + 6.18$	333	68	Atkinson & Pidgeon /22/
$33/7\text{CaO(s)} + 2\text{Al(1)} = 12/7\text{CaO} \cdot \text{Al}_2\text{O}_3 + 3\text{Ca(g)}$	$\log p_{\text{Ca}} = \frac{-10,645}{T} + 9.26$	611	245	Bauer /23/
$6\text{CaO(s)} + 2\text{Al(1)} = 3\text{CaO} \cdot \text{Al}_2\text{O}_3(\text{s}) + 3\text{Ca(g)}$	$\log p_{\text{Ca}} = \frac{-10,670}{T} + 9.27$	613	245	Jacob & Srikanth /24/

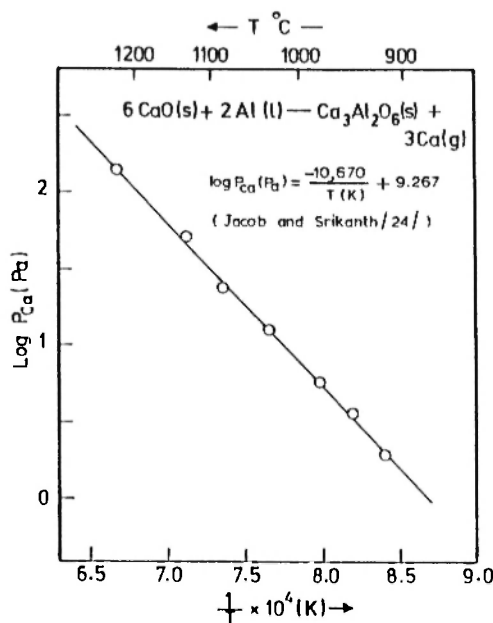


Fig. 8: Experimental calcium vapor pressures corresponding to the reaction $6\text{CaO(s)} + 2\text{Al(l)} \rightarrow 3\text{CaO} \cdot \text{Al}_2\text{O}_3\text{(s)} + 3\text{Ca(g)}$.

entropy changes computed from the vapor pressure measurements of Atkinson and Pidgeon /22/, Bauer /23/ and Jacob and Srikanth /24/ are also compiled in Table 4.

From the known values of the alloy composition corresponding to each equilibrium in the reduction process /20/, knowledge of the activity-composition relationship in liquid Al-Ca alloys at 1373 K and the vapor pressure of pure liquid calcium /4/, the vapor pressure of Ca corresponding to each reduction step can be calculated:

$$p_{\text{Ca}} = a_{\text{Ca}} p_{\text{Ca}}^{\circ} \quad (14)$$

where p_{Ca}° is the vapor pressure of pure liquid calcium and a_{Ca} is the activity of calcium in the alloy at equilibrium. The estimated vapor pressure of calcium for each equilibrium in the reduction process at 1373 K is listed in Table 5 and graphically illustrated in Fig. 9. This figure is of critical importance in the engineering design of the process. At a fixed temperature, the extent of reduction of CaO is determined by the vacuum in the system. A pressure less than the equilibrium value must be maintained to drive the reduction process. When this condition is satisfied, the calcium content of the alloy will be less than the equilibrium value. It follows

therefore that the activity of aluminum in the alloy would be higher than the equilibrium value for the reaction. The aluminum will continue to react with the calcia till physical separation of the reactants retards the process appreciably. The ratio of calcium pressures corresponding to the formation of $3\text{CaO} \cdot \text{Al}_2\text{O}_3$ and $12\text{CaO} \cdot 7\text{Al}_2\text{O}_3$ is ~ 3 . Since a sufficient pressure gradient must be maintained to draw calcium vapor to the condenser, it will be difficult to prevent partial formation of $12\text{CaO} \cdot 7\text{Al}_2\text{O}_3$. Plots similar to Fig. 9 can be constructed at higher temperatures from thermodynamic data. The calculated partial pressure of Ca for the reduction reaction (13) at 1373 K is 30.75 Pa, which compares well with the value of 31.31 Pa at 1373 K obtained from the direct measurements of Jacob and Srikanth /24/. The measurements of Bauer /23/ yield a value of 33.21 Pa at 1373 K for reaction (12). The agreement between the estimated and measured vapor pressures of calcium indicates a good consistency in the thermodynamic data selected for the present analysis. Computations for both equilibrium alloy compositions coexisting with the oxide phases and calcium vapor pressures are in good agreement with the experimental values when the value for the Gibbs energy of formation of CaO

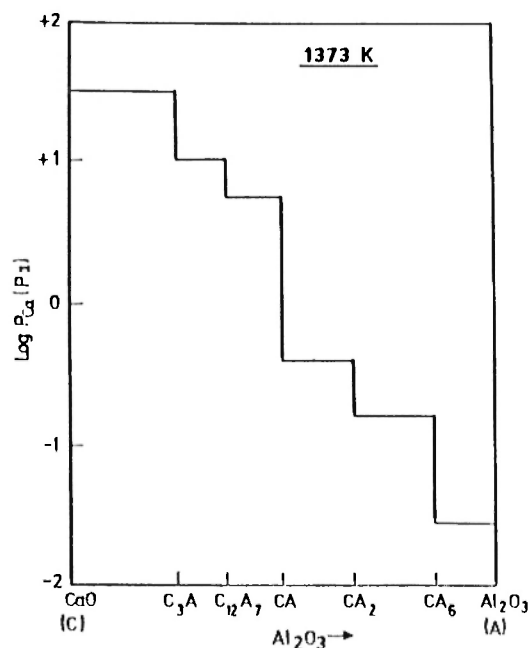


Fig. 9: Equilibrium calcium vapor pressures at 1373 K corresponding to the different end products in the "aluminothermic" reduction of calcia.

at 1373 K is chosen at -487.0 kJ/mol instead of -491.2 kJ/mol given in JANAF /3/. This indicates that the reported value in JANAF /3/ tables may be in error by about 4.2 kJ/mol.

4. CHARGE AND ENTHALPY CALCULATIONS

Recovery of calcium, consumption of aluminum and thermal requirement corresponding to different stages of reduction can be assessed from available data. Recovery can be defined as the ratio of the number of moles of Ca metal to the number of moles of calcium in the charge. The ratio of calcium crown weight per kg of mix to the theoretical crown weight per kg of mix computed assuming complete reaction can be termed efficiency. Mix refers to the briquetting mixture of lime and aluminum powder. Recovery accounts for the loss of calcium as calcium aluminate and is dependent on the stoichiometry of the end product oxide. Efficiency merely refers to the degree of completeness of the reaction and can be as high as 100% when there are no kinetic barriers. When $3\text{CaO}\cdot\text{Al}_2\text{O}_3$ is the end product corresponding to reaction (12):

$$\text{Recovery (\%)} = 3/6 \times 100 = 50\%$$

Calcina required per kg of Ca produced =

$$\frac{2 \times 56.08}{40.08} = 2.8 \text{ kg}$$

Aluminum required per kg of Ca produced =

$$\frac{2 \times 26.98}{3 \times 40.08} = 0.45 \text{ kg}$$

Recoveries of calcium, requirements of aluminum and lime corresponding to the end products $3\text{CaO}\cdot\text{Al}_2\text{O}_3$, $12\text{CaO}\cdot 7\text{Al}_2\text{O}_3$ and $\text{CaO}\cdot\text{Al}_2\text{O}_3$ are summarized in Table 6. The associated enthalpy changes for the different reduction reactions can be determined from a knowledge of the enthalpies of formation of the oxides and enthalpy of vaporization of liquid calcium. The enthalpy of formation of the interoxide compounds in the system $\text{CaO}\text{-}\text{Al}_2\text{O}_3$ were obtained by combining the recommended values of Allibert *et al.* /15/ with the enthalpy of formation of Al_2O_3 from the JANAF table /2/. The enthalpy of formation of CaO was taken as 4.2 kJ/mol more positive than that given in the JANAF compilation /3/ for reasons already discussed. Enthalpy of vaporization of liquid calcium was obtained from the studies of Jacob *et al.* /4/. Thermal requirements for the reduction of calcina for the different end products

TABLE 5
Calculated Equilibrium Vapor Pressures of Calcium for the Various Three-Phase
Equilibria in the System Al-Ca-O at 1373 K

Three-phase equilibrium	p_{Ca} (1373 K) (Pa)
Ca-Al alloy + Al_2O_3 + $\text{CaO}\cdot 6\text{Al}_2\text{O}_3$	0.028
Ca-Al alloy + $\text{CaO}\cdot 6\text{Al}_2\text{O}_3$ + $\text{CaO}\cdot 2\text{Al}_2\text{O}_3$	0.168
Ca-Al alloy + $\text{CaO}\cdot 2\text{Al}_2\text{O}_3$ + $\text{CaO}\cdot\text{Al}_2\text{O}_3$	0.409
Ca-Al alloy + $\text{CaO}\cdot\text{Al}_2\text{O}_3$ + $12\text{CaO}\cdot 7\text{Al}_2\text{O}_3$	5.572
Ca-Al alloy + $12\text{CaO}\cdot 7\text{Al}_2\text{O}_3$ + $3\text{CaO}\cdot\text{Al}_2\text{O}_3$	10.288
Ca-Al alloy + $3\text{CaO}\cdot\text{Al}_2\text{O}_3$ + CaO	30.753

are listed in Table 6. The enthalpy change associated with reduction reaction (13) is found to be 664 kJ in comparison to the value of 613 kJ deduced from the vapor pressure measurements of Jacob and Srikanth /24/. Since the composition of the alloy in equilibrium with CaO and $3\text{CaO}\cdot\text{Al}_2\text{O}_3$ is likely to vary with temperature and may lie in a two-phase field at lower temperatures, the agreement between the theoretical and experimental enthalpy for the reduction reaction is reasonable. Enthalpy and charge calculations have been made using the stoichiometry of the reaction and assuming complete utilization of aluminum. The decrease in the efficiency of utilization of aluminum because of incomplete reaction and calcium losses because of the formation of liquid Al-Ca alloy are ignored.

5. PURITY OF CALCIUM

As the pressure in the reactor is lowered, end products rich in alumina form (Table 5). Alloy-oxide equilibrium studies /20/ indicate that as calcia-deficient end products form, equilibrium concentrations of aluminum in the alloy increase (Fig. 5), resulting in relatively higher aluminum concentrations in the vapor phase and in the condensed metal. The maximum contamination of calcium by aluminum attainable for different degrees of reduction can be calculated from a knowledge of vapor

pressures of liquid aluminum and calcium and activities in liquid Al-Ca alloys, assuming no other contamination. The high volatility of calcium compared to that of aluminum makes possible the extraction of calcium in the process. The ratio of partial pressures of calcium to aluminum is shown in Table 7 for different degrees of reduction resulting in the formation of $\text{CaO}\cdot\text{Al}_2\text{O}_3$, $12\text{CaO}\cdot 7\text{Al}_2\text{O}_3$ and $3\text{CaO}\cdot\text{Al}_2\text{O}_3$. The corresponding purity of calcium obtained by condensing the vapor is also indicated in Table 7. It is seen that the purity is higher when the reaction products contain a high concentration of CaO. If the product is to be used without further distillation, it may be necessary to restrict the reduction of CaO to the first step characterized by the formation of $3\text{CaO}\cdot\text{Al}_2\text{O}_3$. The temperature or vacuum can be controlled to get the desired purity. It is quite likely that some of the aluminum in the vapor phase will condense before it reaches the condenser; hence the actual purity of calcium will be higher than that based on equilibrium thermodynamics.

6. PROCESS CONTROL

It is seen from a physico-chemical point of view that the main process of the reactor control parameters are temperature and pressure of the reactor. The other process control parameters are

TABLE 6
Charge and Thermal Requirements for the "Aluminothermic" Reduction Process
at 1373 K (100% Utilization of Aluminum Assumed)

End Product	Recovery (%)	W_{CaO}^* kg	W_{Al}^{**} kg	Enthalpy of Reaction $\Delta H(\text{kJ/mol of the end product})$
$\text{CaO}\cdot\text{Al}_2\text{O}_3$	75	1.8656	0.4488	662.77
$12/7\text{CaO}\cdot\text{Al}_2\text{O}_3$	64	2.1987	0.4488	679.13
$3\text{CaO}\cdot\text{Al}_2\text{O}_3$	50	2.7984	0.4488	663.89

*CaO consumption per kg of calcium produced

**Al consumption per kg of calcium produced

the particle size of the powders, distribution, porosity of briquettes, surface tension characteristics of the powders, time cycle of reduction and pressure and temperature of the condenser. Design of the reduction reactor and condenser also plays an important role in process optimization. At higher temperatures, the equilibrium vapor pressures of calcium are higher and the demands on the vacuum system are less stringent. Higher temperature improves the driving force for the reaction, reaction rate and heat transfer. As a result, a higher efficiency can be obtained in a restricted time, or the time cycle can be shortened without loss of recovery. However, the life of steel retorts used for the reactor becomes a limiting factor at high temperatures. Temperature of operation is dictated by the comparative economics of shorter retort life versus higher efficiency and/or a shorter cycle. Higher temperatures of operation also result in increased contamination and higher energy inputs. Optimum temperatures of operation are in the range of 1430-1460 K, depending on local conditions. Fig. 9 indicates that the operation of the reactor at higher vacuum levels results in the formation of aluminates deficient in calcium oxide as end products. Thus, at low pressures, recoveries of calcium are considerably enhanced. However, the cost of the high vacuum system and the enhanced time for reduction needed to achieve higher yields, makes such a practice uneconomic. Equilibrium calcium concentrations in liquid Al-Ca alloys are lower when calcia-deficient compounds are formed as end products (Fig. 5). The purity of calcium produced also deteriorates when the pressure in the reactor is lowered sufficiently to form calcia-deficient aluminates.

Briquetting of the mix is recommended in order to provide intimate contact of materials, adequate heat transmission into the charge and ready release of calcium from the charge. The physical quality and density of briquettes are the decisively important factors in this operation. Typical briquetting pressures are of the order of 18.6 mPa and the apparent density of the briquettes is about 2.13-2.29 g/ml; factors such as size or shape of briquettes are probably of far less importance. The physical quality of the briquettes depends on the green strength and thermal shock resistance. Use of fine aluminum powders for reduction will significantly improve the kinetics of reduction, but during reduction the aluminum particles tend to coalesce, leading to slower reaction rates. It has been found that coalescence can be avoided by adding iron powder equal to ~10 wt. percent of aluminum used. Presumably the formation of the iron-aluminum liquid alloy alters the surface tension characteristics in a favorable manner.

The time taken to complete the reduction cycle is an important parameter determining the overall productivity of the plant. Efficiency increases at a diminishing rate as time increases, but productivity decreases at an accelerating rate beyond an optimum value. Therefore, the time per cycle should be chosen to give the best economic combination of recovery and productivity. The time cycle comprises the time for charging, heating of the charge and degassing, energy input and discharging. A major controlling factor is the time required to transfer sufficient heat to the reacting charge to ensure complete reaction of aluminum in the charge. Heat requirements are high because the reaction is endothermic. Either gas or

TABLE 7
Purity and Partial Pressure Ratios for Different End Products

End Product	P_{Ca}/P_{Al}	Purity = $p_{Ca}/(p_{Ca} + p_{Al}) \times 100$
$CaO \cdot Al_2O_3$	10.26	91.12%
$12/7CaO \cdot Al_2O_3$	21.09	95.47%
$3CaO \cdot Al_2O_3$	79.73	98.76%

electric heating can be used. Gas heating should be indirect so that the retorts are not exposed to the combustion products, and, in general, these retort furnaces are fired by producer gas and heated by radiation from a carborundum floor below which combustion takes place. When electrical energy is used, heating may be either external or internal. The charge can be heated internally via resistor elements buried in the charge or located in the evacuated charge chamber by using the charge itself as the resistor, by induction heating of a susceptor within or around the charge mass or by the use of an arc for internal heating in the evacuated chamber. The design of a reactor with internal heating is more complex, and the retort maintenance and operation are more demanding. However, the life of the retort is increased when internal heating is employed. The efficiency of internal electrical heating is more than for gas heating, but this advantage is offset by the high cost of electric power. Time cycles depend on the temperature of reduction, retort size, charge weight, vacuum levels, mix composition and briquette type. Time cycles in industrial practice vary between 8-15 hr.

6.1. Kinetics of the Process

The rate of the process is controlled by a number of factors, of which the most important are:

(i) The difference in the vapor pressure of calcium over the reactants and in the system. This difference is the basic driving force for the reaction. Enhanced pumping rates would result in a more rapid reaction;

(ii) Flux of calcium through the porous briquette and through the retort under the influence of the pressure differential. A reduction in equilibrium partial pressure of calcium adversely affects the rate of diffusion;

(iii) As the reduction proceeds, the reactants must find each other through the accumulating end products. It is difficult to affect a complete reaction unless an excess of aluminum is used in the charge. Normally, 20-30% excess aluminum is used to get high recoveries. Close to 100% efficiency can be achieved by using about 35% excess aluminum, as shown in Fig. 10, if reaction (13) is used as the basis of the calculation. The cost of excess aluminum is offset by the higher yield of calcium. The unreacted aluminum traps some calcium to form an alloy. The small calcium loss on this account is maximum when

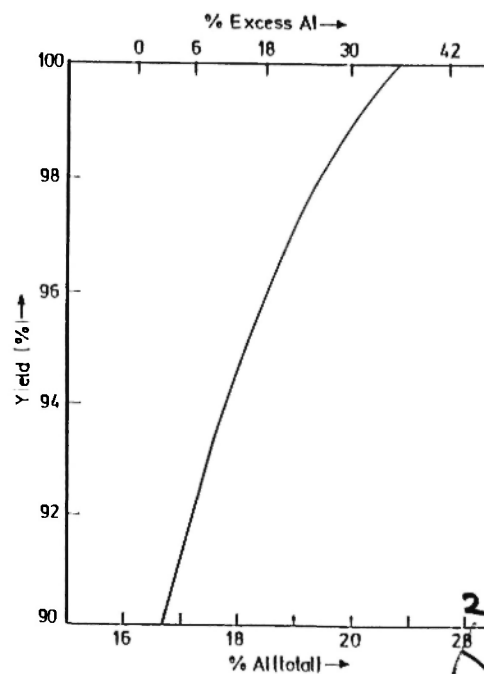


Fig. 10: Yield of calcium as a function of aluminum powder in the mix.

$3\text{CaO} \cdot \text{Al}_2\text{O}_3$ is the reaction product and decreases progressively as calcia-deficient aluminates form;

(iv) The reaction is endothermic and the reactants and products are poor conductors of heat. Heat losses can be minimized by good furnace design, preheating of the charge and reduction of operating temperature.

Any one of the above steps may be rate controlling, and under different conditions a different factor may be rate controlling. In commercial practice it is quite possible that the heat transfer step is rate controlling, emphasizing the importance of furnace design and temperature gradients.

6.2. Plant Practice

A detailed description of the plant practice is beyond the scope of this paper, and only the salient features of the practice will be highlighted. The practice is very similar to the extraction of magnesium. In fact, the same plant can produce both magnesium and calcium. When producing calcium, one uses better vacuum, retorts made of more heat-resistant materials and higher temperature. The various steps which describe the entire process are: (a) charge preparation, (b) retort charging, (c) reduction, (d)

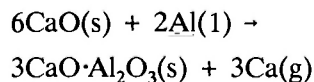
retort discharging and (e) retort blow up.

High purity limestone is calcined to produce lime. The calcined lime is ground, mixed with fine metallic aluminum powders and briquetted. The briquetting operation is normally dry since most of the known binders are harmful to the reaction. Briquetting pressures are of the order of 18.6 mPa, and the resultant apparent density of the briquettes is 2.13 to 2.29 g/ml. Retorts are charged with briquettes to about 80-85% of the retort hot length volume. The retorts are made of Cr-Ni stainless steels. The main process control parameters which characterize the reduction are pressure, temperature and time cycle, as discussed earlier. Operating temperatures are in the range of 1420-1460 K. A rough vacuum or a pull-down vacuum is applied initially to degas and preheat the charge. Subsequently, the high vacuum or holding vacuum is applied. If the retorts are operated at low vacuum levels (~ 15 Pa), mechanical pumps would suffice. However, mercury diffusion pumps backed by mechanical pumps have been used in plant practice [25] where a vacuum of the order of 2.5 Pa has been generated in the retort. Modern mechanical pumping systems can give pressures of the order of 1 Pa. On application of the high vacuum, pressure rapidly drops and calcium vapor starts to evolve. Continuing reaction of the charge is promoted by the mass flow of vapor to the condenser held at a lower temperature and low calcium vapor pressure. Calcium vapor evolves from the charge at an increasing rate, reaches a peak and then diminishes toward the end of the cycle. The rate of chemical reaction can be enhanced by a small addition of CaF_2 to the charge. The retort hardware should be such that the heat losses are minimal, and calcium recoveries are maximal. Radiation shields are inserted between the hot zone and condenser zone of each retort to minimize radiant heat transfer. Condenser sleeves are inserted in the condenser zones immediately behind the radiation shields. Baffle plates are inserted into the cold ends of the condenser sleeves to hold calcium in the sleeves and prevent its escape to the cover plates or vacuum lines. Rubber gasketed cover plates are put in place over the flanged open end of the retorts and are subsequently held in place by a vacuum. The inside wall of the retort hot zone accumulates an adhesive layer of a sticky residue during operation. This is termed as cake build-up and is primarily dependent on the temperature, increasing rapidly as the furnace temperature increases. The presence of a cake layer

in the hot zone serves to make the retort effectively smaller and acts as a serious barrier to heat transmission through the retort wall to the charge. If possible, the cake should be removed before charging the retort. As the retorts are maintained under high vacuum at about 1400 K, the retort walls gradually collapse and have to be restored to shape by inflation or blow up with high pressure air (~ 0.6 mPa). At the end of the reduction cycle, the solid calcium (crown) deposited on the condenser or condenser sleeve is stripped. Collection of calcium in the condenser must be accomplished in a manner that will permit ready removal of the condensate. At low equilibrium calcium vapor pressures, any appreciable back pressure of calcium vapor in the condenser can potentially become a controlling factor which might depress rates of reaction and recovery in a given time. Use of water jacketed condenser heads can prevent the back flow of calcium vapor. The temperature and pressure in the condenser play an important role. To prevent loose, powdery and pyrophoric deposits, the inert gas pressure at the condenser should be relatively low and the condenser temperature reasonably high. A cold condenser encourages the formation of powdery and pyrophoric deposits. A condenser temperature of approximately 800 K appears to be suitable for obtaining crystalline deposits of calcium. The initial deposit during the process tends to be loose because the condenser is cold during this period. The enthalpy released by condensation of the vapor quickly heats the condenser. The thermal load on the condenser is maximum during the peak distillation stage.

7. DISCUSSION AND CONCLUSIONS

From the discussions on the phase stability in the system Al-Ca-O, it is evident that the principle reaction mechanism in the "aluminothermic" reduction of calcium oxide is



Further reduction of $3\text{CaO}\cdot\text{Al}_2\text{O}_3$ in five intermediate stages to Al_2O_3 is possible in vacuum, each equilibrium being characterized by a unique ratio of activity of calcium to aluminum, equilibrium alloy composition and calcium and aluminum partial pressures. Equilibrium partial pressures of calcium

are of the order of 30 Pa at 1373 K and 90 Pa at 1460 K, when the end product is $3\text{CaO}\cdot\text{Al}_2\text{O}_3$. For other calcia-deficient end products, the equilibrium pressures of calcium are progressively lower.

The recovery of calcium is low when the product is rich in calcium oxide. For the end product $3\text{CaO}\cdot\text{Al}_2\text{O}_3$, the percentage recovery is 50%, which increases to 64% for $12\text{CaO}\cdot 7\text{Al}_2\text{O}_3$ and to 75% for $\text{CaO}\cdot\text{Al}_2\text{O}_3$ when the efficiency is 100%. However, the cost of the high vacuum system and the enhanced time of reduction needed to achieve higher recovery of calcium make such a practice uneconomic. The aluminum requirement per unit weight of calcium produced remains unaltered for different reduction reactions. However, the purity of calcium produced deteriorates as the reaction products become deficient in calcia. When $12\text{CaO}\cdot 7\text{Al}_2\text{O}_3$ is the reaction product, the equilibrium pressure of calcium is lower by a factor of ~ 3 . Since a significant pressure gradient must be applied to draw calcium vapor to the condenser, it is difficult to halt completely the formation of $12\text{CaO}\cdot 7\text{Al}_2\text{O}_3$. Use of ~ 35 wt. percent excess aluminum in the mix is necessary to carry the reaction to completion. Low pressures and high temperatures reduce the life of the retort. The calculated enthalpy changes for the different reduction mechanisms are almost equal, indicating that the thermal requirements to produce 1 kg of calcium do not differ much for the end products $3\text{CaO}\cdot\text{Al}_2\text{O}_3$, $12\text{CaO}\cdot 7\text{Al}_2\text{O}_3$ and $\text{CaO}\cdot\text{Al}_2\text{O}_3$. Kinetic considerations indicate that the heat transfer step may be the rate controlling step in commercial practice.

From the above analysis, the best compromise would be to carry the reduction up to the stage where $3\text{CaO}\cdot\text{Al}_2\text{O}_3$ is formed primarily as the end product. Under operating conditions it will be difficult to avoid partial formation of $12\text{CaO}\cdot 7\text{Al}_2\text{O}_3$, since equilibrium pressure for the two stages differs by a factor of only 3.

8. REFERENCES

1. Belitskus, D., *J. of Metals*, **30** (1972).
2. Stull, D.R. and Prophet, H., "JANAF Thermochemical Tables," National Bureau of Standards, U.S. Department of Commerce, Washington (1971).
3. Chase, M.W., Curnutt, J.L., Prophet, H., McDonald, R.A. and Syverud, A.N., *J. Phys. Chem. Ref. Data*, **4**, 1 (1975).
4. Jacob, K.T., Srikanth, S. and Waseda, Y., *Trans. Japan Inst. of Metals*, **29**, 50 (1988).
5. Levin, E.M., Robbins, C.R. and McMurdie, H.F., "Phase Diagram for Ceramists," The American Ceramic Society Inc., Columbus, Ohio (1964).
6. Sommer, F., Lee, J.J. and Predel, B., *Z. Metallkde*, **74**, 425 (1982).
7. Schurmann, E., Funders, P. and Litterscheidt, H., *Archiv. Eisenhutenw.*, **46**, 473 (1975).
8. Chipman, J., in Proc. Sympos. Physical Chemistry of Process Metallurgy, Part I, Interscience Publishers, New York (1961).
9. Rein, R.H. and Chipman, J., *Trans. AIME*, **233**, 415 (1965).
10. Koehler, M.F., Barany, R. and Kelley, K.K., Bureau of Mines, Rept. Invest. RI5711, U.S. Department of Interior, Washington, D.C. (1961).
11. Sharma, R.A. and Richardson, F.D., *J. Iron Steel Inst.*, **198**, 386 (1961).
12. Kor, G.J.W. and Richardson, F.D., *J. Iron Steel Inst.*, **206**, 700 (1968).
13. Carter, P.T. and Macfarlane, T.F., *J. Iron Steel Inst.*, **185**, 54 (1957).
14. Cameron, J., Gibbons, T.B. and Taylor, J., *J. Iron Steel Inst.*, **204**, 1223 (1966).
15. Allibert, M., Chatillon, C., Jacob, K.T. and Lourtau, R., *J. Amer. Ceram. Soc.*, **64**, 307 (1981).
16. Kumar, R.V. and Kay, D.A.R., *Metall. Trans. B*, **16B**, 107 (1985).
17. Brisi, C. and Rolando, P., *Ann. Chim.*, **57**, 1304 (1968).
18. Nurse, R.W., Welch, J.H. and Majumdar, A.J., *Trans. Brit. Ceram. Soc.*, **64**, 409 (1965).
19. Cockayne, B. and Lent, B., *J. Cryst. Growth*, **46**, 467 (1979).
20. Srikanth, S., Srinivasan, V.S., Jacob, K.T. and Allibert, M., *Rev. Intern. des Hautes. Temps. et des Refract.* Submitted for publication.
21. Hultgren, R., Orr, R.L., Anderson, P.D. and Kelly, K.K., "Selected Values of Thermodynamic Properties of Elements," ASM, Metals Park, Ohio (1973).
22. Atkinson, J.T.K. and Pidgeon, L.M., *The Canad. Min. and Metall. Bull.*, Montreal (1948).
23. Bauer, S.L., Ph.D. Thesis, University of Toronto, Canada (1972).
24. Jacob, K.T. and Srikanth, S., *Trans. Ind. Inst. Metals*. Submitted for publication.
25. Loomis, C.C., *Trans. Electrochem. Soc.*, **89**, 207 (1946).